Boltzmann equation for a granular capped rectangle in a thermalized bath of hard disks

H. Gomart,[1] J. Talbot,[2] and P. Viot[1]
[1]*Laboratoire de Physique Théorique des Liquides, Université Pierre et Marie Curie, 4 Place Jussieu, 75252 Paris Cedex, 05 France*
[2]*Department of Chemistry and Biochemistry, Duquesne University, Pittsburgh, PA 15282-1530, USA*
(Received 10 August 2004; published 27 May 2005)

By using the Boltzmann approach, we study the steady-state dynamics of a granular capped rectangle placed in a two-dimensional bath of thermalized hard disks. Hard core collisions are assumed elastic between disks and inelastic between the capped rectangle and the disks, with a normal coefficient of restitution $\alpha<1$. Assuming a Gaussian ansatz for the probability distribution functions, we obtain analytical expressions for the granular temperatures. We show the absence of equipartition and investigate both the role of the anisotropy of the capped rectangle and of the relative ratio of the bath particles to the linear sizes of the capped rectangle. In addition, we investigate a model of a capped rectangle with two normal coefficients of restitution for collisions along the straight and curved surfaces of the capped rectangle. In this case one observes equipartition for a nontrivial ratio of the normal coefficient of restitutions.

DOI: 10.1103/PhysRevE.71.051306 PACS number(s): 45.70.−n, 05.20.-y

I. INTRODUCTION

Granular matter is characterized by the existence of dissipative forces between particles. In order to sustain a collective motion, it is necessary to provide energy continuously. When power supply is sufficiently copious, the assembly of granular particles attains a nonequilibrium steady state (NESS) [1,2]. An important parameter is the granular temperature that is defined as the second moment of the velocity distribution. It is a source of both fascination and inconvenience that the well-known properties of temperatures characterizing thermal systems are not necessarily transferable to granular temperatures. In particular, recent theoretical [2–8] and experimental [9,10] work, has shown that in a binary granular system the two species have different granular temperatures that are nontrivial functions of the microscopic parameters (mass, size, coefficient of restitution,…). Although the absence of equipartition is not surprising for a dissipative system sustained in a NESS, quantitative investigations are necessary since the granular temperatures play an important role in hydrodynamic descriptions of these systems. For example, the absence of equipartition in binary mixtures yields granular temperature gradients which enhance segregation [11]. In addition, the extension of the fluctuation-dissipation theorem is an important issue in the context of granular gases [12]. Other consequences of the absence of equipartition include the ability of a binary system to exhibit a segregation phenomena in a "Maxwell demon" experiment [13]. The reader is also referred to the homogeneous cooling state of a granular mixture [14] and the impurity problem [15].

Most of the above-referenced studies examined assemblies of spherical particles. Yet, in reality, the particles composing granular systems are to some degree anisotropic and, in many cases, strongly so. Even if the particles are smooth, each collision results in some exchange and, possibly, loss of rotational kinetic energy. There are relatively few studies of these systems (but see, for example, Refs. [16–18]) and fewer still that focus specifically on equipartition. Huthmann *et al.* [19] used kinetic theory to examine the free cooling of granular needles in three dimensions and, more recently, two of the present authors studied a two-dimensional system composed of a single granular needle in a thermalized bath of point particles [20] in a NESS. For inelastic needle-point collisions, the rotational granular temperature is smaller than the translational one while both are less than the bath temperature. The validity of the theoretical predictions was confirmed by a comparison with numerical simulations of the model. While this study provided useful insights, the infinitesimal width of the particle is obviously an idealization.

Our objective in the present article is to consider a more realistic system where both the tracer particle and bath particles are of a finite extent. Specifically, we consider a capped rectangle in a bath of thermalized hard disks. Fortunately, despite the increased complexity, it is still possible to obtain an analytic solution of the steady state kinetic equations. The principal difference between the capped rectangle-disk and needle-point systems is that two kinds of collision are possible in the former compared to one in the latter: a disk can collide with either the sides or the caps of the capped rectangle. If each type of collision is characterized by different normal coefficients of restitution, we show that equipartition between the translational and rotational degrees of freedom can be obtained for specific values of these parameters. Consequently, for appropriate ranges of the coefficients of restitution the translational granular temperature may be less than or greater than the rotational one.

II. MODEL AND COLLISION RULES

We investigate a two-dimensional system consisting of a hard capped rectangle of total length $L+2R$, radius R and mass M with a moment of inertia I (the value of which is given in Appendix A). The bath consists of hard disks of mass m and of radius r. Collisions between bath particles are assumed elastic, and the temperature T of the disks remains constant. Conversely, collisions between disks and the capped rectangle are inelastic. In the following, we detail the collision rules that are necessary to develop the kinetic theory.

The vector positions of the center of mass of the capped rectangle and a disk particle are denoted by $\mathbf{r}_1$ and $\mathbf{r}_2$, respectively. The orientation of the capped rectangle is specified by a unit vector $\mathbf{u}_1$ that points along the long axis. Let $\mathbf{r}_{12}=\mathbf{r}_1-\mathbf{r}_2$ and $\mathbf{u}_1^{\perp}$ denote a vector perpendicular to $\mathbf{u}_1$. A collision between a capped rectangle and a disk can take place either on the linear part or on the circular parts of the former. Let O and C denote the center of the capped rectangle and the point of collision, respectively. We define λ as the projection of $\mathbf{OC}$ on the long axis: $\lambda=\mathbf{OC}\cdot\mathbf{u}_1$. At the instant of collision, the quantities just introduced satisfy the following equations:

$$|\mathbf{r}_{12}\cdot\mathbf{u}_1^{\perp}| = (R+r), \tag{1}$$

if $|\lambda|<L/2$, and

$$|\mathbf{r}_{12}\cdot\mathbf{u}_r| = (R+r)+\frac{L\left(|\lambda|-\frac{L}{2}\right)}{2R}, \tag{2}$$

if $R>|\lambda|-L/2>0$, where $\mathbf{u}_r$ denotes the unit vector of the collision axis (see Fig. 1). The relative velocity of the point of contact $\mathbf{V}$ is given by

$$\mathbf{V} = \mathbf{v}_{12} + \boldsymbol{\omega}_1 \times \mathbf{OC}, \tag{3}$$

where $\boldsymbol{\omega}_1$ denotes the angular velocity.

The pre- and post-collisional quantities (the latter are labeled with a prime) satisfy the following:

• Total momentum conservation,

$$M\mathbf{v}'_1 + m\mathbf{v}'_2 = M\mathbf{v}_1 + m\mathbf{v}_2. \tag{4}$$

.

• Angular momentum conservation with respect to the point of contact,

$$I\omega_1'\mathbf{k} = I\omega_1\mathbf{k} + m\mathbf{OC}\times(\mathbf{v}_2-\mathbf{v}'_2), \tag{5}$$

where $\mathbf{k}$ is a unit vector perpendicular to the plane.

As a result of the collision, the relative velocity of the contacting points changes instantaneously according to the following relations:

$$\mathbf{V}'\cdot\mathbf{u}_1^{\perp} = -\alpha\mathbf{V}\cdot\mathbf{u}_1^{\perp}, \tag{6}$$

$$\mathbf{V}'\cdot\mathbf{u}_1 = \mathbf{V}\cdot\mathbf{u}_1, \tag{7}$$

where α is the normal coefficient of restitution.

When the collision occurs on the circular parts of the capped rectangle, the collision rules are given by

$$\mathbf{V}'\cdot\mathbf{u}_r = -\alpha\mathbf{V}\cdot\mathbf{u}_r, \tag{8}$$

$$\mathbf{V}'\cdot\mathbf{u}_\theta = \mathbf{V}\cdot\mathbf{u}_\theta, \tag{9}$$

where $\mathbf{u}_r$ and $\mathbf{u}_\theta$ denote the unit vectors associated with the circular part of the capped rectangle (see Fig. 1(b)) and θ denotes the angle between the direction of the long axis of the capped rectangle and the axis defined by the contact point and the center of the disk.

The tangential coefficient of restitution is set to one for the sake of simplicity. This choice is reflected in the form of Eqs. (7)–(9).

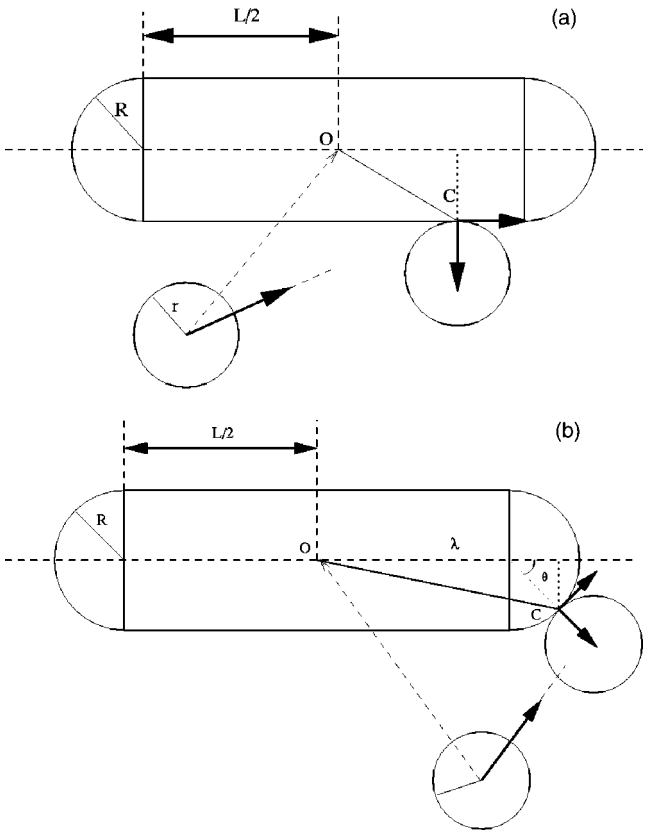

FIG. 1. Geometry of the capped rectangle and a disk in the plane: $\mathbf{r}_{12}$ denotes a vector joining the point labeled 2 and the center of the capped rectangle, λ is the projection of the vector $\mathbf{OC}$ on the long axis of the capped rectangle. (a) Collision between the rectilinear part of the capped rectangle and a disk, $\mathbf{u}_1$ is a unit vector along the long axis of the capped rectangle and $\mathbf{u}_1^{\perp}$ is a unit vector perpendicular to the axis of the capped rectangle. (b) Collision between the circular part of the capped rectangle and a disk. $\mathbf{u}_\mathbf{r}$ and $\mathbf{u}_\theta$ are unit vectors normal and tangential to the surface at the point of contact, respectively.

By combining Eqs. (3)–(6) one obtains, after some algebra, the change of the capped rectangle momentum $\mathbf{\Delta p}=M(\mathbf{v}_1'-\mathbf{v}_1)$ for a collision along the linear part,

$$\Delta\mathbf{p}\cdot\mathbf{u}_1^{\perp} = -\frac{(1+\alpha)\mathbf{V}\cdot\mathbf{u}_1^{\perp}}{\frac{1}{m}+\frac{1}{M}+\frac{\lambda^2}{I}}, \tag{10}$$

for $|\lambda|\leqslant L/2$ and at the two ends of the capped rectangle,

$$\Delta\mathbf{p}\cdot\mathbf{u}_r = -\frac{(1+\alpha)\mathbf{V}\cdot\mathbf{u}_r}{\frac{1}{m}+\frac{1}{M}+\frac{L^2\sin^2\theta}{4I}}, \tag{11}$$

for $R>|\lambda|-L/2>0$ with $\cos\theta=(\lambda-L/2)/R$.

III. KINETIC THEORY

Since we are interested in the homogeneous state, the distribution function $f(\mathbf{v}_1,\omega_1)$ of the capped rectangle obeys the pseudo-Liouville equation,

$$\frac{\partial f(\mathbf{v}_1,\omega_1)}{\partial t} = \int \frac{d\theta_1}{2\pi} \int d\mathbf{v}_2 \int d\mathbf{r}_2 \, \overline{T}_{12} f^{(2)}(\mathbf{v}_1,\omega_1,\mathbf{v}_2), \tag{12}$$

where $f^{(2)}(\mathbf{v}_1,\omega_1,\mathbf{v}_2)$ is the distribution function of the capped rectangle and a disk, and $\overline{T}_{12}$ is the collision operator between a capped rectangle and a disk. The number density of the bath particles n is given by $n=\int d\mathbf{v}_1\, d\omega_1\, d\mathbf{v}_2 f^{(2)}(\mathbf{v}_1,\omega_1,\mathbf{v}_2)$.

Defining the granular temperatures as quadratic average of the appropriate velocity distribution, one has $T_T = M/2\langle \mathbf{v}^2\rangle$ and $T_R = I\langle\omega^2\rangle$ for the translational and rotational granular temperatures, respectively (the angular brackets denote an average with respect to the velocity distribution function of the capped rectangle $f(\mathbf{v}_1,\omega_1)$). By taking the second moment with respect of the velocity and of the angular velocity of Eq. (12), one obtains

$$\frac{2}{M}\frac{\partial T_T}{\partial t} = \int d\mathbf{v}_1 \int d\omega_1 \, \partial_t[\mathbf{v}_1^2 f(\mathbf{v}_1,\omega_1)] = \int \cdots \int d\mathbf{v}_1\, d\omega_1 \frac{d\theta_1}{2\pi} d\mathbf{v}_2\, d\mathbf{r}_2\, \overline{T}_{12} f^{(2)}(\mathbf{v}_1,\omega_1,\mathbf{v}_2)\mathbf{v}_1^2, \tag{13}$$

$$\frac{\partial T_R}{I\,\partial t} = \int d\mathbf{v}_1 \int d\omega_1 \, \partial_t[\omega_1^2 f(\mathbf{v}_1,\omega_1)] = \int \cdots \int d\mathbf{v}_1\, d\omega_1 \frac{d\theta_1}{2\pi} d\mathbf{v}_2\, d\mathbf{r}_2\, \overline{T}_{12} f^{(2)}(\mathbf{v}_1,\omega_1,\mathbf{v}_2)\omega_1^2. \tag{14}$$

In the stationary state the time derivatives of the left-hand side of these two equations are equal to zero.

By considering the integrals, Eqs. (13) and (14) as inner products, the time dependence can be assigned to the dynamical variables, $\mathbf{v}_1$ and ω_1, and this requires the introduction of the adjoint of $\overline{T}_{12}$, T_{12} (for more details, see [21]).

The collision operator between the capped rectangle and a disk, T_{12}, must include the change in quantities (i.e., velocity and angular momentum) produced during the infinitesimal time interval of the collision. This operator is different from zero only if the two particles are in contact and if the particles were approaching just before the collision [22]. For a collision between a disk and the rectilinear part of the capped rectangle, the explicit form of the operator, given by

$$T_{12} \propto \Theta(L/2-|\lambda|)\,\delta(|\mathbf{r}_{12}\cdot\mathbf{u}_1^{\perp}| - r - R) \times \left|\frac{d|\mathbf{r}_{12}\cdot\mathbf{u}_1^{\perp}|}{dt}\right| \Theta\left(-\left|\frac{d|\mathbf{r}_{12}\cdot\mathbf{u}_1^{\perp}|}{dt}\right|\right)(b_{12}-1), \tag{15}$$

where b_{12} is an operator that changes pre-collisional quantities to post-collisional quantities and $\Theta(x)$ is the Heaviside function, and for a collision at two ends of the capped rectangle,

$$T_{12} \propto \Theta(R+L/2-|\lambda|)\Theta(|\lambda|-L/2) \times \delta\left(|\mathbf{r}_{12}\cdot\mathbf{u}_r| - \left(r+R+\frac{L}{2R}\left(|\lambda|-\frac{L}{2}\right)\right)\right) \times \left|\frac{d|\mathbf{r}_{12}\cdot\mathbf{u}_r|}{dt}\right| \Theta\left(-\left|\frac{d|\mathbf{r}_{12}\cdot\mathbf{u}_r|}{dt}\right|\right)(b_{12}-1). \tag{16}$$

.

The others terms of the collision operator correspond to the necessary conditions of contact $\Theta(L/2-|\lambda|)\delta(|\mathbf{r}_{12}\cdot\mathbf{u}_1^{\perp}| - (r+R))$, and approach $\Theta(-|d|\mathbf{r}_{12}\cdot\mathbf{u}_1^{\perp}|/dt|)$ in the first case and $\Theta(R+L/2-|\lambda|)\Theta(|\lambda|-L/2)\delta(|\mathbf{r}_{12}\cdot\mathbf{u}_r| - [r+R+(L/2R)(|\lambda|-L/2)])$, and approach $\Theta(-|d|\mathbf{r}_{12}\cdot\mathbf{u}_r|/dt|)$ in the second case.

In order to obtain a tractable solution we invoke the assumption of molecular chaos that allows the factorization of two particle distribution function,

$$f^{(2)}(\mathbf{v}_1,\omega_1,\mathbf{v}_2) = f(\mathbf{v}_1,\omega_1)\Phi(\mathbf{v}_2), \tag{17}$$

where $f(\mathbf{v}_1,\omega_1)$ is the angular and translational velocity distribution function of the capped rectangle and $\Phi(\mathbf{v}_2)$ is the velocity distribution function of a disk. This assumption is valid in the limit of low density and corresponds to the Boltzmann approximation.

By taking the second moments of the distribution function of the capped rectangle and after substitution of the collision operator (Eq. (15)), one obtains explicitly for the translational kinetic energy,

$$\begin{aligned}\int \cdots \int d\mathbf{r}_2\, d\mathbf{v}_1\, d\mathbf{v}_2\, d\omega_1\, d\theta_1 \Bigg[& \Theta(L/2-|\lambda|)\,\delta(|\mathbf{r}_{12}\cdot\mathbf{u}_1^{\perp}| - (r+R)) \left|\frac{d|\mathbf{r}_{12}\cdot\mathbf{u}_1^{\perp}|}{dt}\right| \Theta\left(-\left|\frac{d|\mathbf{r}_{12}\cdot\mathbf{u}_1^{\perp}|}{dt}\right|\right) \\ & \times f(\mathbf{v}_1,\omega_1)\Phi(\mathbf{v}_2)\Delta E_1^T + \Theta(R+L/2-|\lambda|)\Theta(|\lambda|-L/2) \\ & \times \delta\left(|\mathbf{r}_{12}\cdot\mathbf{u}_r| - \left[r+R+\frac{L}{2R}\left(|\lambda|-\frac{L}{2}\right)\right]\right) \\ & \times \left|\frac{d|\mathbf{r}_{12}\cdot\mathbf{u}_r|}{dt}\right| \Theta\left(-\left|\frac{d|\mathbf{r}_{12}\cdot\mathbf{u}_r|}{dt}\right|\right) f(\mathbf{v}_1,\omega_1)\Phi(\mathbf{v}_2)\Delta E_1^T\Bigg] \\ & = 0. \end{aligned} \tag{18}$$

where Delta E_1^T is the energy change of the capped rectangle during a collision with a both disk.

A similar equation can be written for rotational kinetic energy. Since the impulse of the collision depends on the location of the impact, it is easy to show that the solution is not a Gaussian, a property already observed in the model of a needle and points [20]. However, the actual distribution is expected to be close to Gaussian, if the normal coefficient of restitution is not too small. Moreover, when the anisotropy of the granular particle goes to zero, one recovers the results obtained by Martin and Piasecki [2], i.e., the velocity distribution is exactly Gaussian for all values of the normal coefficient of restitution. Conversely, when the anisotropy is very large, one approaches the needle-point system for which we

showed (by simulation) that the deviation from a Gaussian distribution is quite small, even for coefficients of restitution of 0.2 [20].

Since the deviations from the Maxwell distribution are small, we use it as a trial function. That is, we assume that

$$f(\mathbf{v}_1,\omega_1) \propto \exp\left(-\frac{M\mathbf{v}_1{}^2}{2\gamma_T T}-\frac{I\omega_1^2}{2\gamma_R T}\right), \tag{19}$$

where γ_T and γ_R are the ratios of the translational and rotational capped rectangle temperatures to the bath temperature T, respectively. The velocity distribution function $\Phi(\mathbf{v}_2)$ of bath particles is given exactly by

$$\Phi(\mathbf{v}_2) \sim \exp\left(-\frac{m\mathbf{v}_2^2}{2T}\right), \tag{20}$$

since bath particles interact by elastic collisions.

In summary, in order to obtain the granular temperatures of the capped rectangle, it is necessary to (i) calculate the change of translational and rotational energy occurring during a collision; (ii) perform an average over all degrees of freedom of the collision integral.

IV. CALCULATION AND RESULTS

A. Energy changes during a collision

When a disk collides with the capped rectangle, the change of the translational kinetic energy of the latter is given by

$$\begin{aligned}\Delta E_1^T &= \frac{M}{2}((\mathbf{v}_1')^2-(\mathbf{v}_1)^2)\\ &= \Delta\mathbf{p}\cdot\mathbf{v}_1+\frac{1}{M}\frac{\Delta\mathbf{p}^2}{2}\\ &= -(1+\alpha)\frac{\mathbf{V}\cdot\mathbf{u}_1^{\perp}\mathbf{v}_1\cdot\mathbf{u}_1^{\perp}}{\frac{1}{m}+\frac{1}{M}+\frac{\lambda^2}{I}}+\frac{1}{2M}\frac{(1+\alpha)^2(\mathbf{V}\cdot\mathbf{u}_1^{\perp})^2}{\left(\frac{1}{m}+\frac{1}{M}+\frac{\lambda^2}{I}\right)^2},\end{aligned} \tag{21}$$

for $|\lambda|<L/2$, and

$$\Delta E_1^T = -\frac{(1+\alpha)\mathbf{V}\cdot\mathbf{u}_r\mathbf{v}_1\cdot\mathbf{u}_r}{\frac{1}{m}+\frac{1}{M}+\frac{L^2\sin^2\theta}{4I}}+\frac{1}{2M}\frac{(1+\alpha)^2(\mathbf{V}\cdot\mathbf{u}_r)^2}{\left(\frac{1}{m}+\frac{1}{M}+\frac{L^2\sin^2\theta}{4I}\right)^2}. \tag{22}$$

for $R>|\lambda|-L/2>0$.

The collision also results in a change of rotational energy, for $|\lambda|<L/2$,

$$\begin{aligned}\Delta E_1^R &= \frac{I}{2}((\omega_1')^2-(\omega_1)^2)\\ &= -\frac{\lambda(1+\alpha)}{2}\frac{\mathbf{V}\cdot\mathbf{u}_1^{\perp}(\omega_1'+\omega_1)}{\frac{1}{m}+\frac{1}{M}+\frac{\lambda^2}{I}}\\ &= -\lambda(1+\alpha)\frac{\mathbf{V}\cdot\mathbf{u}_1^{\perp}\omega_1}{\frac{1}{m}+\frac{1}{M}+\frac{\lambda^2}{I}}+\frac{\lambda^2(1+\alpha)^2(\mathbf{V}\cdot\mathbf{u}_1^{\perp})^2}{2I\left(\frac{1}{m}+\frac{1}{M}+\frac{\lambda^2}{I}\right)^2},\end{aligned} \tag{23}$$

and for $R>|\lambda|-L/2>0$,

$$\begin{aligned}\Delta E_1^R = &-(1+\alpha)\frac{L\sin\theta\mathbf{V}\cdot\mathbf{u}_r\omega_1}{2\left(\frac{1}{m}+\frac{1}{M}+\frac{L^2\sin^2\theta}{4I}\right)}\\ &+\frac{(1+\alpha)^2L^2\sin^2\theta(\mathbf{V}\cdot\mathbf{u}_r)^2}{8I\left(\frac{1}{m}+\frac{1}{M}+\frac{L^2\sin^2\theta}{4I}\right)^2}.\end{aligned} \tag{24}$$

B. Granular temperatures

After inserting Eqs. (19) and (20) in Eq. (18) it is necessary to perform integrations over each variable in the corresponding equation for the rotational energy. Details of this rather technical task are given in Appendix B. After some tedious calculation, one obtains the following set of equations:

$$b[cI_1^{01}(a,k)+(1-c)J_1^{01}(a,k)] = \frac{1+\alpha}{2}[cI_2^{03}(a,k)+(1-c)J_2^{03}(a,k)], \tag{25}$$

$$a[cI_1^{11}(a,k)+(1-c)J_1^{11}(a,k)] = \frac{1+\alpha}{2}[cI_2^{13}(a,k)+(1-c)J_2^{13}(a,k)], \tag{26}$$

where

$$k=\frac{L^2}{4I\left(\frac{1}{m}+\frac{1}{M}\right)}, \tag{27}$$

$$a=\gamma_R\frac{M+m}{M+m\gamma_T}, \tag{28}$$

$$b=\gamma_T\frac{M+m}{M+m\gamma_T}. \tag{29}$$

and

$$c=\frac{L/2}{L/2+(r+R)} \tag{30}$$

and I_m^{np} and J_m^{np} are given by

$$I_m^{np}(u,v) = \int_0^1 dx \frac{x^{2n}(1+uvx^2)^{p/2}}{(1+vx^2)^m}, \tag{31}$$

$$J_m^{np}(u,v) = \int_0^{\pi/2} d\theta \sin^{2n}(\theta) \frac{(1+uv\sin^2\theta)^{p/2}}{(1+v\sin^2\theta)^m}. \tag{32}$$

Explicit expressions for the integrals appearing in Eqs. (25) and (26) are given in Appendix C. Equation (26) is an implicit equation for a that, for a given value of α, can be solved with standard numerical methods. b is then easily obtained by calculating the ratio of integrals of Eq. (25). Finally, from the values of a and b, γ_T and γ_R can be obtained from Eqs. (28) and (29).

A first check is the elastic case, $\alpha=1$, for which one obtains $a=b=1$ which gives $\gamma_T=1$ and, since $a/b=\gamma_R/\gamma_T$, $\gamma_R=1$, i.e., the temperatures of translational and rotational degrees of freedom are the same and correspond to the bath temperature, a property of an equilibrium system.

In the limit $R\to 0$ and $r\to 0$, for which $c\to 1$ corresponding to a needle in a bath of point particles, one recovers the results of Ref. [20]. More interesting is the limit $R\to 0$ with r remaining finite, i.e., a needle in a bath of *disks*. By using Eq. (30) one obtains that $c=L/(L+2r)$. Since $c<1$, unlike the simple needle-point system, there is a contribution resulting from collisions between bath particles and the needle's tips. This type of collision is dominant when the bath particles are larger than the longest dimension of the anisotropic particle.

To illustrate the effect of this contribution, Figs. 2(a) and 2(b) compare the system of a needle in a bath of point particles and the system of a needle in a bath of disks, the radius of disks r are equal to $L/4$ in Fig. 2(a) and $r=9L/2$ in Fig. 2(b). It is noticeable that the translational and rotational temperatures of the latter system are smaller than those of the needle in a bath of points, an effect that becomes more pronounced when the radius of the disks becomes larger than the length of the needle.

The difference $\gamma_T-\gamma_R$ is shown in the insets for the needle and the bath of points and for the needle and the bath of disks. Note that the translational temperature is always larger than the rotational temperature and that the difference depends very weakly on the size of the radius of the bath particle. Additionally, the difference increases when the coefficient of restitution decreases from 1 (elastic case), reaches a maximum for a value of $\alpha\sim 0.3$ and decreases slightly when the coefficient of restitution decreases further.

Figure 3 shows the influence of the anisotropy of the tracer particle. The rotational temperature is always lower than the translational temperature whatever the elongation of the particles, but the effect is greater when the elongation is large. The two upper curves correspond the translational (full curve) and rotational (dashed curve) temperature of the capped rectangle when $L=R$, the two intermediate curves to granular temperatures when $L=3R$, and the two lower curves for a capped rectangle with $L=10R$.

When the anisotropy of the capped rectangle approaches zero, i.e., $L/R\to 0$, $c\to 0$, one can show by using Eqs. (25) and (26) that

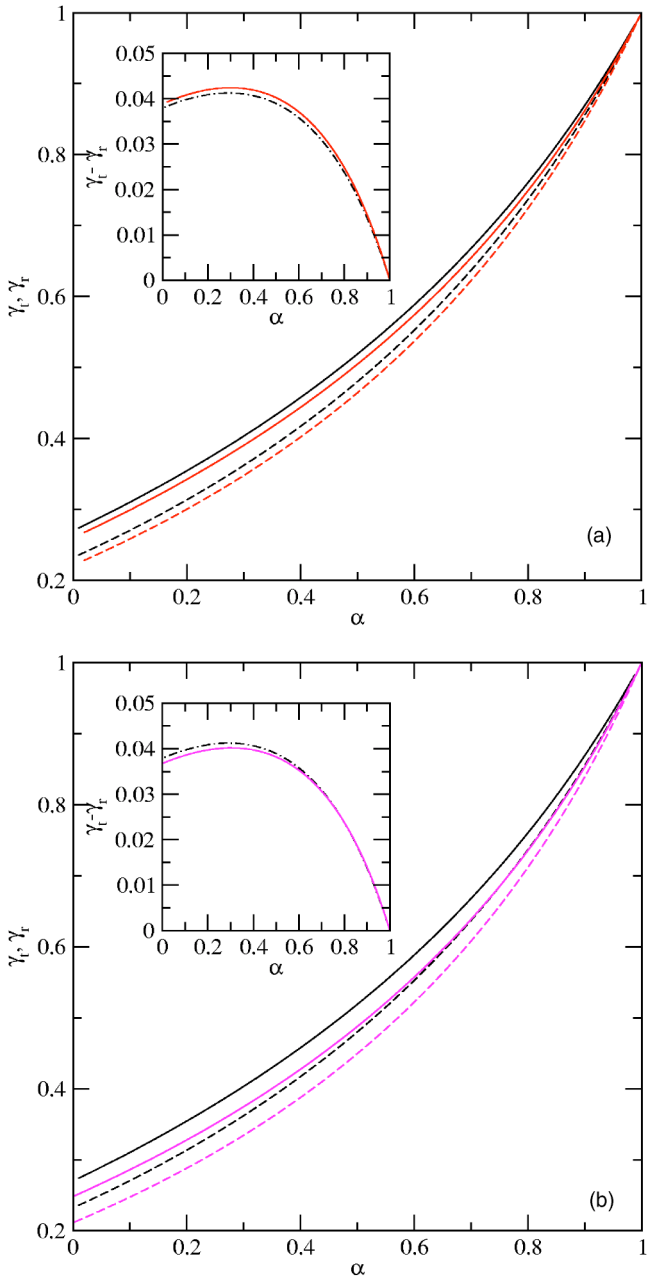

FIG. 2. Ratio of the translational (full curve) γ_T and rotational γ_R (dashed curve) granular temperature to the temperature of the bath versus the normal coefficient of restitution α for a system of a needle and a bath of points and a system of a needle and a bath of disks for $c=2/3$ (a) and for $c=1/10$. The curves corresponding to the needle-point system are always above those for the needle-disk system (b). The insets display the differences $\gamma_T-\gamma_R$ vs α for the needle in the bath of disks (full curve) and the needle in the bath of points (dashed curve).

$$\gamma_T = \frac{1+\alpha}{2+\frac{m}{M}(1-\alpha)}, \tag{33}$$

which is the the result of Martin and Piasecki [2] for a spherical tracer particle in a bath of spherical particles.

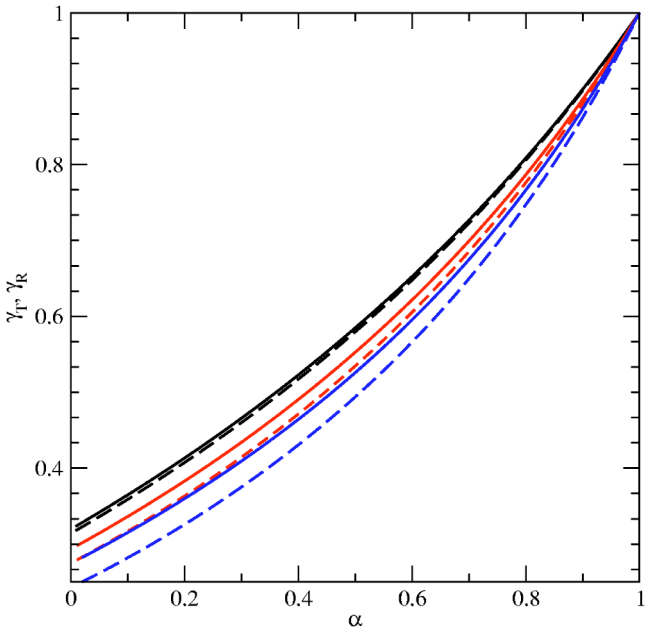

FIG. 3. Ratio of the translational (full curve) γ_T and rotational γ_R (dashed curve) granular temperature to the temperature of the bath versus the normal coefficient of restitution α for a capped rectangle and a bath of disks $r=R$, for different values of the anisotropy, $L=R, 3R, 10R$, top to bottom in each group.

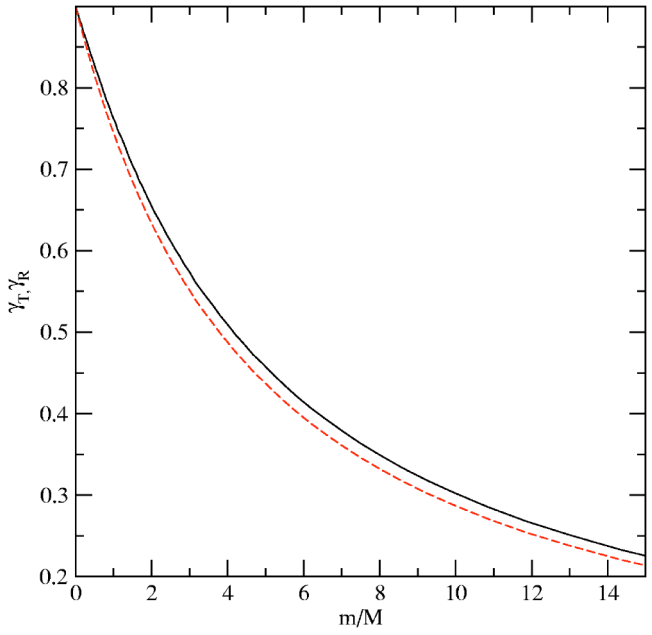

FIG. 4. Ratio of the granular temperatures γ_T (full curve) γ_R (dashed curve) to the bath temperature as a function of the mass ratio m/M, for a homogeneous capped rectangle with $c=4/7$.

Moreover, the limit $L/R \to 0$ leads ro equipartition between the rotational and translational granular temperatures, a result which is different from a model of pure spherical particles where, in the absence of tangential friction, the particles cannot exchange rotational energy. In physical systems, the particles are never completely spherical and our model shows that if an infinitesimal amount of anisotropy is present, the translational and rotational temperatures are equal in the steady state. Although our analysis provides no quantitative information about the relaxation time to reach this NESS, it is likely to be very long in this limit of small anisotropy.

C. Influence of mass ratio

We consider a homogeneous capped rectangle of mass M in a bath of disks each of mass m for which $M \neq m$. When $m/M \to 0$ one obtains, from Eqs. (25) and (26), that

$$\gamma_T = \gamma_R = \frac{1+\alpha}{2}, \tag{34}$$

i.e., equipartition between the degrees of freedom of the tracer particle, but not between the bath and the tracer particle. This is, moreover, the same result for a needle in a bath of point particles.

We conjecture that this result is general in the sense that we expect equipartition between the different degrees of freedom of the tracer particle in a bath of light particles, whatever the shape of the tracer particle and the dimension of the system. The behavior for finite values of the ratio m/M is shown in Fig. 4. The granular temperatures decrease when the ratio m/M increases, and the translational temperature remains higher than the rotational temperature for each value of α.

V. NONUNIFORM COEFFICIENT OF RESTITUTION

In practice it may be difficult to construct a capped rectangle for which the coefficient of restitution is constant over the entire perimeter. It is clear, for example, that if the object is composed of a homogeneous viscoelastic material, collisions with the ends will be characterized by a smaller coefficient of restitution than collisions with the linear part. This effect becomes more pronounced as the elongation (L/R) increases. Other possibilities exist for a nonhomogeneous capped rectangle composed of two or more materials. For example, a hard material may be used to construct the caps. In addition, the coefficient of restitution could depend on the relative velocity of the point of impact [23], an effect that one neglects here as a first approximation.

As a first approach to describe this possibility, we consider in this section a capped rectangle where the coefficient of restitution is equal to α_1 for a collision along the rectilinear part of the object and equal to α_2 for one along the circular part: see Fig. 5. Using the procedure outlined above one obtains the following set of closed equations:

$$b((1+\alpha_1)cI_1^{01}(a,k) + (1+\alpha_2)(1-c)J_1^{01}(a,k)) = \frac{(1+\alpha_1)^2}{2}cI_2^{03}(a,k) + \frac{(1+\alpha_2)^2}{2}(1-c)J_2^{03}(a,k), \tag{35}$$

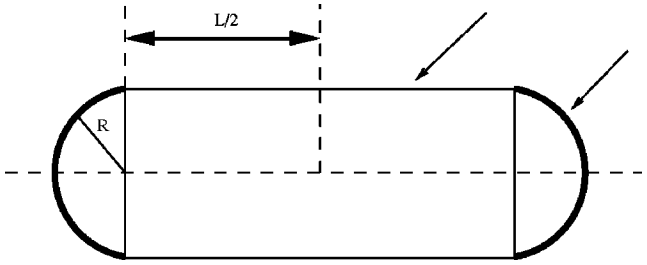

FIG. 5. Sketch of the capped rectangle with two coefficients of restitution α_1 (rectilinear part) and α_2 (circular part).

$$a((1+\alpha_1)cI_1^{11}(a,k)+(1+\alpha_2)(1-c)J_1^{11}(a,k)) = \frac{(1+\alpha_1)^2}{2}cI_2^{13}(a,k)+\frac{(1+\alpha_2)^2}{2}(1-c)J_2^{13}(a,k). \tag{36}$$

Figure 6 shows the ratio of translational and rotational temperature of a capped rectangle with $R=r$ and $L=2R$ to the temperature of the bath as a function of the normal coefficient of restitution α_2 with a fixed $\alpha_1=0.5$. One notes that the translational temperature becomes smaller than the rotational temperature for $\alpha_2>0.765$. When the two curves cross, equipartition is recovered, but unlike the limiting cases discussed above of a capped rectangle with a uniform coefficient of restitution (light bath particles, infinitely small anisotropy), for a nontrivial value of coefficient of restitution α_2 and, moreover, for larger values of α_2 the ratio of temperatures is inverted.

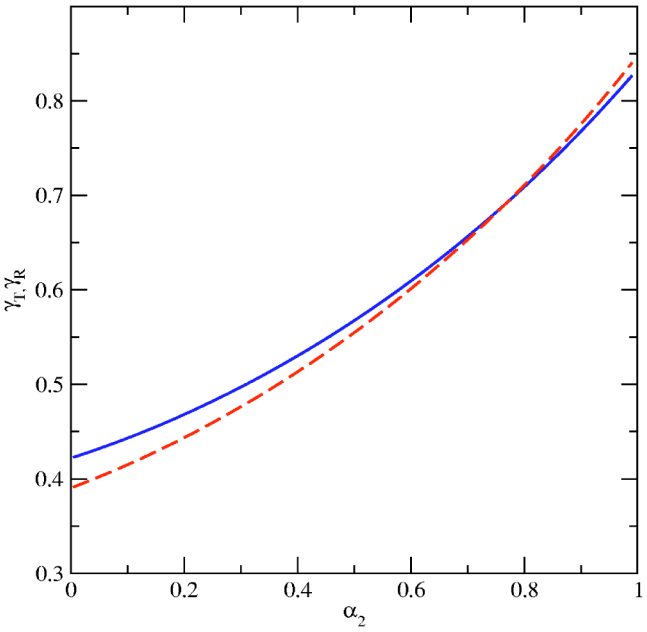

FIG. 6. Ratio of the translational (full curve) γ_T and rotational γ_R (dashed curve) granular temperature to the temperature of the bath versus the normal coefficient of restitution α_2 with a normal coefficient of restitution $\alpha_1=0.5$ for a homogeneous capped rectangle with $M=m$, $L=2R$ and $R=r$. Note that equipartition is recovered for a nontrivial value of α_2.

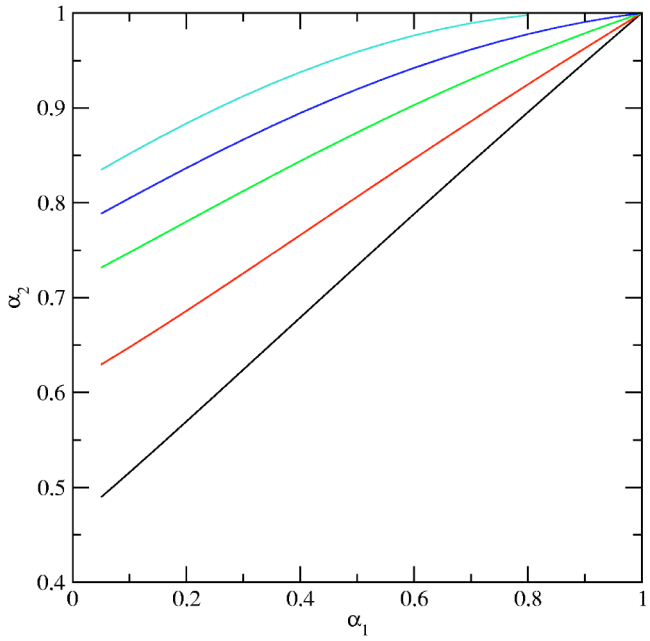

FIG. 7. α_1 vs α_2 where equipartition is obtained for $r=R$ and different values of $L=R,2R,\ldots,5R$ from bottom to top.

One can determine in general when equipartition is recovered for a capped rectangle with two coefficients of restitution. Using the relation $a=b$ (assumption of equipartition) and Eqs. (35) and (36), one obtains two implicit equations with the three parameters α_1, α_2 and a. A simple numerical procedure allows us to obtain α_2 as a function of α_1.

Figure 7 shows the equipartition lines in the (α_1,α_2) space. Above each line, corresponding to a given elongation of the rectangle, $T_R>T_T$ while the reverse inequality applies to the region below the line. It is noticeable that as the elongation increases, the region of the (α_1,α_2) space where $T_R>T_T$ decreases.

Figure 8 shows the role of the size of the bath particles on the existence of equipartition of a capped rectangle of length $L=8R$. For small bath particles, only a small range of α_1 (between 0 and $\sim$0.3) with a smaller range of α_2 (between $\sim$0.89 and 1) allows equipartition for the tracer particle. For larger bath disks, all values of α_1 (between 0 and 1) are available with a smaller corresponding range of α_2.

VI. CONCLUSION

We have investigated the influence of the anisotropy of a tracer particle in a bath of thermalized disks in two dimensions. By using a mean-field approach, we have obtained analytical results for the rotational and translational temperatures. For a homogeneous capped rectangle with a uniform normal restitution coefficient, the translational temperature is always higher than the rotational temperature, with the difference depending on the elongation of the tracer particle, the size of the bath particles and the mass ratio.

At present, the exact dependence of the coefficient of restitution on the position of the point of impact is unknown. It seems likely, however, that it is not constant along the pe-

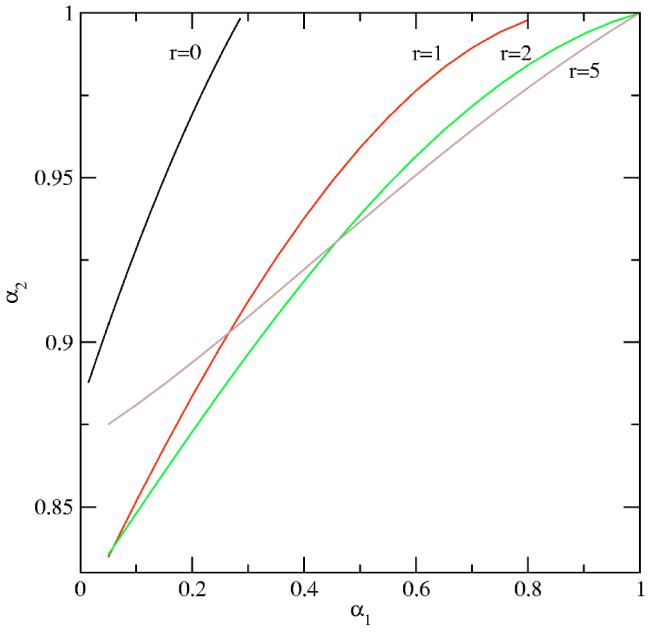

FIG. 8. α_1 vs α_2 where equipartition is obtained for $L=8R$ and for different values of disk radius $r/R=0,1,2,3,5$ (number labeling each curve).

rimeter. As a first approximation, we considered an extension of the model where it takes on two values: one for collisions with the linear part and another for collisions with the caps. In this case the difference between the translational and rotational granular temperatures can be either positive or negative depending on the values of the coefficients of restitution and the other parameters. It is clearly possible to generalize the calculation to allow for a continuously varying restitution coefficient and an arbitrary convex body.

It would also be interesting to investigate a system of a tracer particle with a small anisotropy where the tangential coefficient of restitution has a nontrivial value $(-1<\alpha_T<1)$ where the limits correspond to a perfectly rough and a perfectly smooth surface, respectively. The intermediate situation corresponds to some friction which is important in some granular systems.

APPENDIX A: MOMENT OF INERTIA

For a homogeneous capped rectangle, the moment of inertia is given by

$$I_{Oz} = \int \int_S \rho(x^2 + y^2)dx\,dy, \tag{A1}$$

and the mass of the system is

$$M = \int \int_S \rho\,dx\,dy = \rho(\pi R^2 + 2LR), \tag{A2}$$

which gives

$$I_{Oz} = \rho R\left\{\pi R\left[\frac{R^2}{2} + \left(\frac{L}{2}\right)^2\right] + \frac{2}{3}L\left[3R^2 + \left(\frac{L}{2}\right)^2\right]\right\}. \tag{A3}$$

By substituting the density as a function of the total mass of the capped rectangle,

$$I = M\left[\frac{\frac{2L\left(3R^2 + \left(\frac{L}{2}\right)^2\right)}{3} + \pi R\left(\frac{R^2}{2} + \left(\frac{L}{2}\right)^2\right)}{\pi R + 2L}\right]. \tag{A4}$$

Two well-known limits are recovered,

$$\lim_{R\to 0} I_{Oz} = \frac{ML^2}{12}, \tag{A5}$$

$$\lim_{L\to 0} I_{Oz} = \frac{MR^2}{2}. \tag{A6}$$

For an inhomogeneous capped rectangle, the moment of inertia depends on the mass distribution. However, it is possible to determine the lower and upper bounds for allowable values.

A trivial lower bound of zero is obtained when the mass is concentrated at the center. Conversely, when the mass is distributed equally at the two extremities of the object (point masses of $M/2$ at a distance of $L+R$ from the center on each side), one obtains

$$I = M(L/2 + R)^2, \tag{A7}$$

which gives the upper bound for the moment of inertia.

APPENDIX B: NEEDLE AVERAGE ENERGY LOSS

As for binary mixtures of spheres [4], we use a Gaussian ansatz for the distribution functions and introduce two different temperatures corresponding to the translational and rotational degrees of freedom of the needle [24].

The homogeneous distribution functions of the needle and of the points are then given, respectively, by Eqs. (19) and (20)

We introduce the vectors $\boldsymbol{\chi}$ and $\boldsymbol{\nu}$ such that

$$\boldsymbol{\chi} = \frac{1}{\sqrt{2T(M\gamma_T + m)}}(M\mathbf{v}_1 + m\mathbf{v}_2), \tag{B1}$$

$$\boldsymbol{\nu} = \sqrt{\frac{mM}{2T(M\gamma_T + m)\gamma_T}}(\mathbf{v}_1 - \gamma_T\mathbf{v}_2). \tag{B2}$$

The scalar products $\mathbf{V}\cdot\mathbf{u}_1^{\perp}$ and $\mathbf{V}\cdot\mathbf{u}_r$ can be expressed as

$$\mathbf{V}\cdot\mathbf{u}_1^{\perp} = h\left[(\gamma_T - 1)\chi\cdot\mathbf{u}_1^{\perp} + \sqrt{\gamma_T}\left(\sqrt{\frac{m}{M}} + \sqrt{\frac{M}{m}}\right)\boldsymbol{\nu}\cdot\mathbf{u}_1^{\perp}\right] + \omega_1\lambda, \tag{B3}$$

$$\mathbf{V}\cdot\mathbf{u}_r = h\left[(\gamma_T-1)\chi\cdot\mathbf{u}_r + \sqrt{\gamma_T}\left(\sqrt{\frac{m}{M}}+\sqrt{\frac{M}{m}}\right)\boldsymbol{\nu}\cdot\mathbf{u}_r\right] + \omega_1\frac{L}{2}\sin\theta, \tag{B4}$$

where $h=\sqrt{2T/(M_\gamma T+m)}$.

Let us introduce $\xi=\omega_1\sqrt{I/2T_\gamma R}$. The translational energy loss is given by the formula

$$\sum_{p=\pm1}\left[\int d\lambda\int\frac{d\theta_1}{2\pi}\int d\chi\int d\nu\int d\xi\exp(-\chi^2-\nu^2-\xi^2),\right.$$
$$|\mathbf{V}\cdot\mathbf{u}_1^\perp|\Theta(p\mathbf{V}\cdot\mathbf{u}_1^\perp)\Theta\left(\frac{L}{2}-|\lambda|\right)\Delta E_1^T + (R+r)$$
$$\times\int d\theta\int\frac{d\theta_1}{2\pi}\int d\chi\int d\nu\int d\xi\exp(-\chi^2-\nu^2-\xi^2)$$
$$\left.\times|\mathbf{V}\cdot\mathbf{u}_r|\Theta(p\mathbf{V}\cdot\mathbf{u}_r)\Delta E_1^T\right]=0. \tag{B5}$$

Since Eq. (B3) depends only on $\boldsymbol{\chi}\cdot\mathbf{u}_1^\perp$ and $\boldsymbol{\nu}\cdot\mathbf{u}_1^\perp$, one can freely integrate over the direction of $\mathbf{u}_1$ for the vectors $\boldsymbol{\chi}$ and $\boldsymbol{\nu}$, and similarly for Eq. (B4). The integration over θ_1 can be easily performed.

We introduce the three-dimensional vectors $\mathbf{G}_{\mathbf{u}_1^\perp}$ and $\mathbf{s}_{\mathbf{u}_1^\perp}$ with components:

$$\mathbf{G}_{\mathbf{u}_1^\perp}=(G_1,G_2,G_3), \tag{B6}$$

$$=\left(h(\gamma_T-1),h\sqrt{\frac{\gamma_T}{mM}}(m+M),\lambda\sqrt{\frac{2T\gamma_R}{I}}\right), \tag{B7}$$

and

$$\mathbf{s}_{\mathbf{u}_1^\perp}=(s_1,s_2,s_3), \tag{B8}$$

$$=(\chi\cdot\mathbf{u}_1^\perp,\nu\cdot\mathbf{u}_1^\perp,\xi). \tag{B9}$$

Respectively, one has to introduce $\mathbf{G}_{\mathbf{u}_r}$ and $\mathbf{s}_{\mathbf{u}_r}$ vectors associated with collisions on the circular parts of the capped rectangle by changing $\mathbf{u}_1^\perp$ in $\mathbf{u}_r$ and λ by $(L/2)\sin\theta$. By inserting Eq. (21) in Eq. (B5), the average energy loss can be rewritten as

$$\sum_{p=\pm1}\int_{-L/2}^{L/2}d\lambda\int d\mathbf{s}_{u_1^\perp}\exp(-\mathbf{s}_{u_1^\perp}^2)|\mathbf{G}_{u_1^\perp}\cdot\mathbf{s}_{u_1^\perp}|\Theta(p\mathbf{G}_{u_1^\perp}\cdot\mathbf{s}_{u_1^\perp})$$
$$\times\left[\frac{1}{2M}\frac{(1+\alpha)^2(\mathbf{G}_{u_1^\perp}\cdot\mathbf{s}_{u_1^\perp})^2}{\left(\frac{1}{m}+\frac{1}{M}+\frac{\lambda^2}{I}\right)^2}\right.$$
$$\left.-\frac{(1+\alpha)\mathbf{G}_{u_1^\perp}\cdot\mathbf{s}_{u_1^\perp}}{\frac{1}{m}+\frac{1}{M}+\frac{\lambda^2}{I}}h\left(\gamma_T s_1+\sqrt{\frac{m\gamma_T}{M}}s_2\right)\right]+(R+r)$$
$$\times\int_0^{2\pi}d\theta\int d\mathbf{s}_{u_r}\exp(-\mathbf{s}_{u_r}^2)|\mathbf{G}_{u_r}\cdot\mathbf{s}_{u_r}|\Theta(p\mathbf{G}_{u_r}\cdot\mathbf{s}_{u_r})$$
$$\times\left[\frac{1}{2M}\frac{(1+\alpha)^2(\mathbf{G}_{u_r}\cdot\mathbf{s}_{u_r})^2}{\left(\frac{1}{m}+\frac{1}{M}+\frac{L^2\sin^2\theta}{4I}\right)^2}-\frac{(1+\alpha)\mathbf{G}_{u_r}\cdot\mathbf{s}_{u_r}}{\frac{1}{m}+\frac{1}{M}+\frac{L^2\sin^2\theta}{4I}}\right.$$
$$\left.\times h\left(\gamma_T s_1+\sqrt{\frac{m\gamma_T}{M}}s_2\right)\right]=0. \tag{B10}$$

By defining a new coordinate system in which the z axis is parallel to $\mathbf{G}$, one finds that the integrals of Eq. (B10) involve Gaussian integrals of the form

$$\int d\mathbf{s}\exp(-\mathbf{s}^2)(|\mathbf{G}|s_z)^2\Theta(\pm s_z)G_i s_z=\frac{\pi}{2}|\mathbf{G}|^2G_i \tag{B11}$$

and

$$\int d\mathbf{s}\exp(-\mathbf{s}^2)(|\mathbf{G}|s_z)^3\Theta(\pm s_z)=\frac{\pi}{2}|\mathbf{G}^3|, \tag{B12}$$

which finally leads to Eq. (25). The equation for rotational energy is derived following exactly the same procedure.

APPENDIX C: INTEGRALS

The coupled equations (25) and (26) depend on the eight integrals $I_1^{01}(a,k)$, $I_2^{03}(a,k)$, $I_1^{11}(a,k)$, $I_2^{13}(a,k)$ [24], $J_1^{01}(a,k)$, $J_2^{03}(a,k)$, $J_1^{11}(a,k)$, $J_2^{13}(a,k)$ which can be expressed in terms of transcendental and special functions. For completeness, we give below their expressions,

$$I_1^{01}(a,k)=\sqrt{\frac{a}{k}}\ln(\sqrt{ak}+\sqrt{1+ak})+\sqrt{\frac{1-a}{k}}\arctan\left(\sqrt{\frac{(1-a)k}{1+ak}}\right), \tag{C1}$$

$$I_2^{03}(a,k)=\frac{a^{3/2}}{\sqrt{k}}\ln(\sqrt{ak}+\sqrt{1+ak})+\frac{(1-a)\sqrt{1+ak}}{2(1+k)}+\frac{1+a-2a^2}{2\sqrt{k(1-a)}}\arctan\left(\sqrt{\frac{(1-a)k}{1+ak}}\right), \tag{C2}$$

$$I_1^{11}(a,k)=\frac{\sqrt{ak+1}}{2k}+\frac{1-2a}{2\sqrt{a}k^{3/2}}+\ln(\sqrt{ak}+\sqrt{1+ak})-\frac{\sqrt{1-a}}{k^{3/2}}\arctan\left(\sqrt{\frac{(1-a)k}{1+ak}}\right), \tag{C3}$$

$$I_2^{13}(a,k)=\frac{\sqrt{1+ak}(ak-1+2a)}{2k(k+1)}+\frac{\sqrt{a}(3-4a)}{2k^{3/2}}\ln(\sqrt{ak}+\sqrt{1+ak})+\frac{\sqrt{1-a}(1-4a)}{2k^{3/2}}\arctan\left(\sqrt{\frac{(1-a)k}{1+ak}}\right), \tag{C4}$$

$$J_1^{01}(a,k) = aK(\sqrt{-ak}) + (1-a)\Pi(-k,\sqrt{-ak}), \quad \text{(C5)}$$

where $K(x)$ and $\Pi(x,y)$ denote the complete elliptic integral of the first kind and the incomplete elliptic integral of the third kind, respectively,

$$J_2^{03}(a,k) = \left(a^2 - \frac{(1-a)^2}{2(k+1)}\right)\frac{K\left(\sqrt{\frac{ak}{(1+ak)}}\right)}{\sqrt{(1+ak)}} + \frac{(1-a)\sqrt{(1+ak)}}{2(k+1)}E\left(\sqrt{\frac{ak}{1+ak}}\right) + \frac{(1-a)(2ak+a+k+2)}{2(k+1)^2\sqrt{(1+ak)}}\Pi\left(\frac{k}{k+1},\sqrt{\frac{ak}{1+ak}}\right), \quad \text{(C6)}$$

where $E(x)$ denotes the complete elliptic integral of the second kind,

$$J_1^{11}(a,k) = -\frac{a}{k\sqrt{(1+ak)}}K\left(\sqrt{\frac{ak}{1+ak}}\right) + \frac{\sqrt{1+ak}}{k}E\left(\sqrt{\frac{ak}{1+ak}}\right) - \frac{1-a}{k(k+1)\sqrt{(1+ak)}}\Pi\left(\frac{k}{k+1},\sqrt{\frac{ak}{1+ak}}\right), \quad \text{(C7)}$$

and, finally,

$$J_2^{13}(a,k) = \frac{1+2ak-3a^2-4a^2k}{2k(k+1)\sqrt{1+ak}}K\left(\sqrt{\frac{ak}{1+ak}}\right) + \frac{\sqrt{1+ak}(2ak+3a-1)}{2k(k+1)}E\left(\sqrt{\frac{ak}{1+ak}}\right) + \frac{k+4a^2k-3a+3a^2-5ak}{2k(k+1)^2\sqrt{(1+ak)}}\Pi\left(\frac{k}{k+1},\sqrt{\frac{ak}{1+ak}}\right). \quad \text{(C8)}$$

[1] S. McNamara and S. Luding, Phys. Rev. E **58**, 2247 (1998).
[2] P. A. Martin and J. Piasecki, Europhys. Lett. **46**, 613 (1999).
[3] V. Garzó and J. Dufty, Phys. Rev. E **60**, 5706 (1999).
[4] A. Barrat and E. Trizac, Granular Matter **4**, 57 (2002).
[5] S. R. Dahl, C. M. Hrenya, V. Garzó, and J. W. Dufty, Phys. Rev. E **66**, 041301 (2002).
[6] R. Clelland and C. M. Hrenya, Phys. Rev. E **65**, 031301 (2002).
[7] J. Montanero and V. Garzó, Mol. Simul. **29**, 357 (2003).
[8] M. Alam and S. Luding, J. Fluid Mech. **476**, 69 (2003).
[9] K. Feitosa and N. Menon, Phys. Rev. Lett. **88**, 198301 (2002).
[10] R. D. Wildman and D. J. Parker, Phys. Rev. Lett. **88**, 064301 (2002).
[11] J. Galvin, S. R. Dahl, and C. M. Hrenya, J. Fluid Mech. **528**, 207 (2005).
[12] A. Barrat, V. Loreto, and A. Puglisi, Physica A **334**, 513 (2004).
[13] A. Barrat and E. Trizac, Mol. Phys. **101**, 1713 (2003).
[14] A. Santos and J. W. Dufty, Phys. Rev. E **64**, 051305 (2001).
[15] A. Santos and J. W. Dufty, Phys. Rev. Lett. **86**, 4823 (2001).
[16] T. Pöschel, J. Phys. I **5**, 1431 (1995).
[17] I. S. Aranson and L. S. Tsimring, Phys. Rev. E **67**, 021305 (2003).
[18] T. Mullin (private communication).
[19] M. Huthmann, T. Aspelmeier, and A. Zippelius, Phys. Rev. E **60**, 654 (1999).
[20] P. Viot and J. Talbot, Phys. Rev. E **69**, 051106 (2004).
[21] T. V. Noije, M. H. Ernst, and R. Brito, Physica A **251**, 266 (1998).
[22] T. Aspelmeier, T. M. Huthmann, and A. Zippelius, "Free cooling of particles with rotational degrees of freedom," in *Granular Gases* (Springer-Verlag, Berlin, 2001), p. 31.
[23] R. Ramirez, T. Pöschel, N. V. Brilliantov, and T. Schwager, Phys. Rev. E **60**, 4465 (1999).
[24] The integrals I_1^{01}, I_2^{03}, I_1^{11} and I_2^{13} corrrespond to the integrals I_1, I_2, I_3 and I_4 of Ref. [20] respectively. The expressions of I_2 and I_3 have some typos in Ref. [20] and the correct integrals are displayed here.